The Response of Composite Ecosystem Services to Urbanization: From the Perspective of Spatial Relevance and Spatial Spillover

Zhenyue Liu, Pengyan Zhang, Guanghui Li, Dan Yang, and Mingzhou Qin

***Abstract*—Ecosystems offer a wide array of benefits to support human livelihoods and enhance the quality of life. Quantitative evaluation of ecosystem services (ESs) is crucial for achieving the goal of sustainable development. The Yellow River Basin has a large population, and there are contradictions and conflicts in ecological protection, resource utilization, and economic development, among which the downstream region is the most prominent. However, the ESs selected in the existing research are not comprehensive enough, and there are also few studies that further focus on the effects of urbanization on this basis. This article calculated seven types of ESs based on the InVEST model and related methods, and then constructed a composite ecosystem service index (CESI), and studied its spatiotemporal evolution and response to urbanization indicators through bivariate spatial autocorrelation and spatial metrological models. We found that from 1990 to 2020, the CESI fluctuated and decreased with time, with a significant positive spatial correlation but showed a weakening trend. There were differences in the evolution process of the spatial correlation between the CESI and population density, economic density, and land development degree, but ultimately the spatial correlation changed from positive to negative. In terms of spatial spillover effect, population density had a significant positive effect on the CESI, land development had a significant negative effect, and economic density had a weak spillover effect. This article provides a certain reference basis for governments at all levels to formulate relevant strategies for environmental protection and economic development.**

***Index Terms*—Affected areas of the lower Yellow River (AALYR), bivariate spatial autocorrelation, ecosystem services (ESs), spatial Durbin model (SDM), spatial spillover.**

Manuscript received 26 July 2023; revised 13 August 2023; accepted 24 August 2023. Date of publication 1 September 2023; date of current version 13 September 2023. This work was supported in part by the National Natural Science Foundation of China under Grant 41601175 and Grant 41801362, in part by the Program for Innovative Research Talent in University of Henan Province under Grant 20HASTIT017, in part by the Funding for the Construction of the Key Laboratory for Agricultural Nonpoint Source Pollution Control on the Huang-Huai-Hai Plain in 2023, under Grant 2023HNNPSCL-HNDX001, and in part by the 2022 Program for Youth Talent of Zhongyuan. *(Corresponding authors: Pengyan Zhang; Mingzhou Qin.)*

Zhenyue Liu, Guanghui Li, and Dan Yang are with the College of Geography and Environmental Science, Henan University, Kaifeng 475004, China (e-mail: liuzhenyue@henu.edu.cn; gh-li@henu.edu.cn; Yangdan219@henu.edu.cn).

Pengyan Zhang is with the College of Urban Economics and Public Management, Capital University of Economics and Business, Beijing 100070, China, and also with Xinyang Vocational and Technical College, Xinyang 464000, China (e-mail: pengyanzh@126.com).

Mingzhou Qin is with the College of Geography and Environmental Science, Henan University, Kaifeng 475004, China, and also with Henan Overseas Expertise Introduction Center for Discipline Innovation (Ecological Protection and Rural Revitalization Along the Yellow River), Henan University, Kaifeng 475004, China (e-mail: mzqin@henu.edu.cn).

Digital Object Identifier 10.1109/JSTARS.2023.3311107

I. Introduction

THE climate problem with global warming as the main symbol is the major problem facing mankind in the 21st century, which has caused a negative impact on the economy, society, and ecological environment of all countries [1], [2], [3]. Climate change affects the way species interact with each other and their habitats, thus changing the products and services they provide to human society [4]. Ecosystem services (ESs) are all kinds of ecological products or services that human beings obtain from the ecosystem and its ecological process directly or indirectly, which can provide strong support for ecological planning management and environmental protection decision making [5]. However, the expansion of built-up land and population concentration caused by rapid urbanization has brought huge pressure on the ecosystem [6]. Once the external interference exceeds the acceptable level, it may cause problems, such as habitat degradation and biodiversity reduction. The contradiction between the high demand for ESs and the degradation of ESs caused by urbanization is increasingly prominent [7]. Therefore, ESs have attracted more and more attention from scholars and become one of the hot research topics in the world.

The research on ESs mainly includes the classification, assessment, and impact factors of ESs. The classification of ESs can be carried out from two aspects: function classification and value classification. The initial research is to classify ESs based on their own functions. Later, in order to evaluate the value of ESs, the function is gradually transformed into corresponding economic value for classification [8]. In terms of function classification, many scholars have proposed different types of classification. For example, Costanza is divided into 17 types [9], and De Groot is divided into 4 categories and 23 subclasses [8]. In terms of value classification, scholars have also conducted a lot of discussions. Most of them believe that ecosystem service value (ESV) includes use value and nonuse value, which can be further subdivided into direct use value, indirect use value, existence value, and heritage value [10], [11]. Based on the classification of ESs, researchers have carried out various ESV assessments at different scales, such as global [12], national [13], and regional [14]. In addition to converting it into economic value for evaluation, researchers have also developed evaluation models, such as Integrated Valuation of Ecosystem Services and Tradeoffs (InVEST), ARIES, and SoLVES for material quality evaluation [15]. Among them, the InVEST model has

been widely used because of its many evaluation modules and more perfect development. It can quickly and accurately evaluate the regional ESs and can well perform spatial visualization [16], [17]. These studies are mainly on the supply side of ESs. Scholars have also gradually focused on the demand side of regional ESs [18]. Some scholars have selected Ess, such as food supply [19] and water conservation [20], and calculated their supply and demand relationship, and then evaluate the level of regional ESs. Based on ESs assessment, some scholars will analyze its influencing factors. The research shows that the decisive factor of ES change is land use [21], and socioeconomic factors and natural factors are also the key factors affecting ESs change. Socioeconomic factors include population [22], economy [23], urbanization [24], and policy [25], and natural factors include terrain [26], temperature, precipitation, and other climatic factors [27]. Through sorting out the existing studies, it is found that the ESs assessment is mostly based on a single service or a selection of multiple services to measure separately. Building a composite ecosystem service index (CESI) for regional ESs assessment is the main transformation direction of current research. Compared with previous studies, this article selects more comprehensive ESs to construct the CESI and analyzes its response relationship with urbanization from both spatial and quantitative perspectives.

China is undergoing an extensive and rapid urbanization process. The rapid growth of population, expansion of urban areas, and socioeconomic development have led to an increasing demand for ESs, which has seriously affected the ecosystem and its related services [28]. Therefore, it is necessary to measure the regional composite ESs capacity and explore the impact of urbanization to provide a support basis for formulating reasonable and targeted ecological environment protection and construction measures. There are great differences in natural resource endowments, population scale, and socioeconomic among different regions, resulting in different ecological and environmental situations. Among them, the quality of the ecological environment in the Yellow River Basin is directly related to the evolution trend of China's ecological security [29], [30]. The ecological protection and high-quality development of the Yellow River Basin have become an important national strategy; therefore, the ecological protection of the Yellow River Basin is currently a hot research topic [31]. The population in the basin is mainly distributed in the lower reaches, and the economic development is relatively fast. The rapid urbanization in the lower reaches of the Yellow River Basin has made significant contributions to the overall socioeconomic development of the basin, but it has also exacerbated land-use/land cover changes and had a significant impact on the ecological environment [32]. It is necessary to evaluate the ESs of the region and analyze its response to the urbanization process. Based on this, we take the affected areas of the lower Yellow River (AALYR) as the study area, aiming at building a CESI to evaluate the ESs function and its space–time evolution characteristics; and exploring the spatial correlation between urbanization indicators and CESI, and deeply analyzing the spatial effect of urbanization indicators (see Fig. 1). On this basis, it is expected to provide decision-making reference for promoting the high-quality development of the Yellow River Basin. At the same time, some major river basins in the world also face the same problem of coordinating ecological protection and urbanization. Therefore, the results of this article can also provide a theoretical reference for the development of other similar regions.

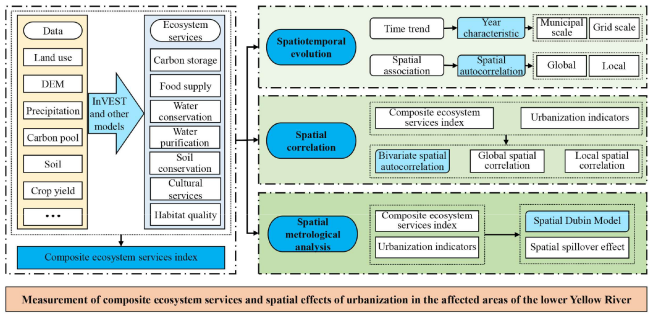

Fig. 1. Research framework.

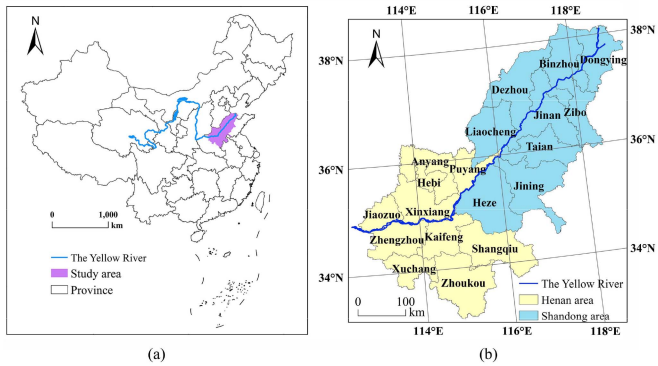

Fig. 2. Overview of the study area.

II. Materials and Methods

A. Study Area

The lower reaches of the Yellow River have a total length of 785.6 km and a total drop of 93.6 m, and a wide and flat river course across the North China Plain. The landform is dominated by plains, hills, and estuarine deltas. Therefore, the river slope is small and the water flow is gentle, which leads to serious siltation of the river and the gradual elevation of the riverbed. The region is also one of the major grain-producing areas in the country. It is one of the most important areas for agricultural production and economic development in China. Considering the ancient flood diversion, the agricultural irrigation needs, and the integrity of the traditional irrigation areas and administrative divisions of the Yellow River, this article defines the AALYR as 19 prefecture-level cities, with a total area of 148 100 km^2 [33], [34] (see Fig. 2). In 2020, the population of the study area reached 125 million, the total GDP was 7.43 trillion yuan, and the average urbanization rate was 58.60%. The process of urbanization was advancing rapidly.

B. Data Sources

Based on related methods, we calculated the ESs of the AALYR from 1990 to 2020 and collected data from the following

TABLE I
DATA ATTRIBUTES AND SOURCES

Name	Source	Type	Accuracy
Land use GDP density Population density	Resource and Environment Science and Data Center of Chinese Academy of Sciences	Raster data	1 km×1 km
Annual potential evapotranspiration Average monthly temperature	Loess plateau science data center, National Earth System Science Data Sharing Infrastructure, National Science and Technology Infrastructure of China [35], [36]	NETCDF	-
Nighttime light data	A Big Earth Data Platform for Three Poles [37]	Raster data	1 km×1 km
DEM	Geospatial data cloud	Raster data	30 m×30 m
Average annual precipitation	National Climate Data Center	Site data	-
Soil database	FAO	Raster data	1 km×1 km
Crop yield, sown area, and price	Statistical yearbooks	Statistical data	-
Carbon pool	Model guide and pieces of literature [38], [39], [40]	Constant	-

sources, according to the input parameters required by each module (see Table I).

Among them, land-use data are constructed through manual visual interpretation using Landsat remote sensing images as the main source of information. According to the classification criteria of the website, it is divided into six categories and used as the basic data for the calculation of the InVEST model. Population density and GDP density data are spatial grid data generated through spatial interpolation based on their spatial interaction with land-use data, nighttime light remote sensing data, and residential density data, respectively. The DEM data adopt advanced spaceborne thermionic emission and antiradiometer (ASTER) GDEM V2 data product, which is calculated and generated based on the "ASTER" data, and is the high-resolution elevation image data covering the global land surface. The ordinary kriging interpolation method was used to convert meteorological station data into spatial distribution data and export it as a resolution of 1 km × 1 km of grid data. Raster data were processed by "Extract by Mask" to obtain the data of the study area. Subsequently, operations, such as "resample," "zonal statistics," and "reclassify," were carried out to ensure that all types of raster data meet the needs of the model. The degree of land development was obtained by calculating the proportion of built-up land in the administrative area using land-use data, and rainfall erosion factor, soil erodibility factor, habitat sensitivity data, and other parameters were calculated through the model guide and based on the above data.

In terms of selecting indicators to reflect urbanization, nighttime light remote sensing data have been proven to be effective in quantifying the level of urbanization [41]. And we want to further decompose urbanization into population urbanization, economic urbanization, and land urbanization. Therefore, after processing the nighttime lighting data through "zonal statistics," we calculated the Pearson correlation coefficients between it and population density, GDP density, and land development level

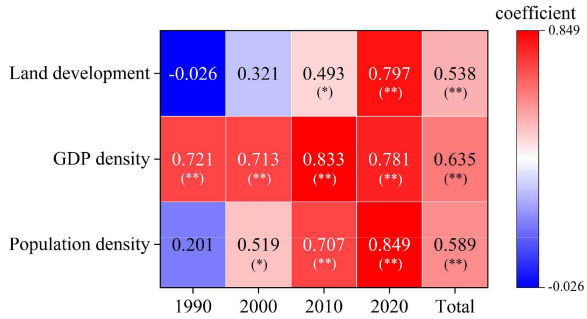

Fig. 3. Pearson correlation coefficients between nighttime lighting data and three indicators. ($^{*}P < 0.05$, that is, passing the test at the 5% significance level; $^{**}P < 0.01$, that is, passing the test at the 1% significance level.).

(see Fig. 3). The results showed that the overall correlation between them was significant. Although the early correlation between population density and land development level was not significant, the correlation gradually became significant over time. It is appropriate to use population density, GDP density, and land development degree to reflect the level of urbanization.

C. Methods

1) InVEST: The InVEST model is a set of model systems to evaluate ES functions and their economic values [42]. The InVEST model includes 20 main modules. This study used the corresponding modules to quantify the following five types of ESs: carbon storage, water conservation, water purification, soil conservation, and habitat quality.

According to the classification of land use, the carbon storage module provides statistics on the carbon density. It calculates the sum to obtain the carbon storage of the region. The calculation formula is [43]

$$C_t = C_a + C_b + C_s + C_d \tag{1}$$

where C_t is the total carbon storage of the basin, C_a is the above-ground part, C_b is the underground part, C_s is the soil part, and C_d is the dead organic part. Considering the availability of data, this study only considered the following carbon pools: the above-ground part, underground part, and soil.

The water conservation module estimates the water supply based on the water balance. The main algorithm is [44]

$$Y_{xj} = \left[1 - \frac{\mathrm{AET}_{xj}}{P_x}\right] \times P_x \tag{2}$$

where Y_{xj} is the annual water supply in unit x in landscape type j (mm), AET_{xj} is the annual actual evapotranspiration, and P_x is the annual precipitation

$$\frac{\mathrm{AET}_{xj}}{P_x} = \frac{1 + \omega_x + R_{xj}}{1 + \omega_x + R_{xj} + 1/R_{xj}} \tag{3}$$

where $\frac{\mathrm{AET}_{xj}}{P_x}$ is the ratio of actual evapotranspiration to precipitation, R_{xj} is the Budyko dryness index on grid x, and ω_x represents the ratio of the annual water demand of vegetation to precipitation

$$\omega_x = Z \times (AWC_x/P_x) \tag{4}$$

$$R_{xj} = (k_{xj} \times eto_x)/P_x \tag{5}$$

where Z is an empirical constant reflecting the seasonal characteristics of regional precipitation and is obtained according to the model guidelines; AWC_x is the plant water content of the grid; eto_x is the potential evapotranspiration; and k_{xj} is the ratio of crop evapotranspiration ET to potential evapotranspiration eto_x in different development stages.

The water purification module usually uses N and P nutrient retention and output to characterize the degree of water purification. The model was developed in two steps. First, the annual average runoff for each plot was calculated using the model water conservation module. Then, the pollutant interception in each landscape plot was obtained based on the annual average runoff. The calculation formula is given as follows [45]:

$$ALV_x = HSS_x \times POL_x \tag{6}$$

where ALV_x is the modified load value of x grid, HSS_x is the hydrological sensitivity, and POL_x is the output coefficient.

The soil conservation calculates the soil erosion amount based on the nature and vegetation protection and the actual soil erosion amount. The formula is [46]

$$SD = RKLS - USLE \tag{7}$$

where SD is the soil conservation amount, $USLE$ is the actual soil erosion amount, and $RKLS$ is the potential soil erosion amount.

Quality is reflected by the size of the index in the range [0, 1]. A higher value corresponds with better habitat quality. The calculation formula is [47]

$$Q_{xj} = H_j \left[1 - \left(\frac{D_{xj}^z}{D_{xj}^z + k^z}\right)\right] \tag{8}$$

where Q_{xj} refers to the habitat quality; H_j refers to the habitat suitability; D_{xj} refers to the stress level; and k refers to the semisaturation coefficient.

2) Other Modules: The food supply module is mainly based on food produced by different land-use types [48]. It mainly includes grains, oil plants, vegetables, fruits, and meat, and combines the calories and edible proportions of various foods to convert food output into energy. The calculation formula is given as follows:

$$FS_x = \sum_{k=1}^{K} \sum_{c=1}^{C} A_{ckx} \times FS_{ckx} \tag{9}$$

where FS_x is the total food energy provided by area x, A_{ckx} is the area of food c in grid x (hm^2), and FS_{ckx} is the supply of the corresponding food c per unit area ($\mathrm{kJ{\cdot}hm^{-2}}$). According to (9) and the specific meaning represented by each parameter, the supply of food c per unit area in a certain area can be calculated as follows:

$$FS_{ckx} = \frac{FS_x}{\sum_{k=1}^{K}\sum_{c=1}^{C} A_{ckx}} = \frac{Y_c \times E_c}{\sum_{k=1}^{K}\sum_{c=1}^{C} A_{ckx}} \tag{10}$$

where Y_c is the output of different food types, E_c is the calorie content of different foods, and the other variables are the same as those in (9).

Cultural services are not calculated using the InVEST model but are instead based on the cultural service value equivalent [49]. The formula is

$$CS_j = E \times VC_j \tag{11}$$

where CS_j is the cultural service value, E is the ESV equivalent factor, and VC_j is the cultural service value equivalent.

3) Analytic Hierarchy Process (AHP): The AHP is a multilevel weight analysis and decision-making method. It is a simple, flexible, scientific, and practical method and can simplify complex problems. Therefore, it is widely used in multiobjective and hierarchical decision making [50], [51]. AHP can be used to determine the subjective weight of each evaluation indicator as follows.

First, a hierarchical structure is built using yaahp software (https://www.metadecsn.com/). According to people's recognition of the importance of each factor, a 1–9 scale method is used to assign each factor to construct a judgment matrix.

Second, the subjective weight Wi of indicators is calculated as follows.

1) The consistency indicator CI can be obtained by

$$CI = \frac{\lambda_{\max} - n}{n - 1}. \tag{12}$$

2) The average random consistency index is determined according to the RI value.
3) The consistency ratio CR is

$$CR = \frac{CI}{RI}. \tag{13}$$

When $CR < 0.1$, it indicates that the consistency is reasonable; otherwise, it is unreasonable, and the consistency check must be performed again.

4) Spatial Autocorrelation: Spatial autocorrelation analysis can reveal whether the distribution of spatial variables is related to adjacent variables [52]. In this study, we analyzed the spatial

TABLE II
JUDGMENT MATRIX OF THE GENERAL OBJECTIVE LEVEL FOR EACH RELATED FACTOR OF THE ELEMENT

Name	*Wi*	λ_{max}	CR
Carbon storage	0.0925		
Food supply	0.3076		
Water conservation	0.1325		
Water purification	0.0270	7.4048	0.0491<0.1
Soil conservation	0.1148		
Cultural services	0.0247		
Habitat quality	0.3009		

correlation of CESI and its spatial response to the urbanization indicators. The calculation method was given as follows [53]:

$$I = \frac{\sum_{i=1}^{n}\sum_{j=1}^{n} W_{ij}\left(x_i - \bar{x}\right)\left(y_j - \bar{y}\right)}{S^2 \sum_{i=1}^{n}\sum_{j=1}^{n} W_{ij}} \tag{14}$$

where I is the spatial autocorrelation index; n is the number of space units; W_{ij} is the spatial weight matrix; x_i and y_j are the observed values; and S^2 is the variance.

The local Moran's I is

$$I_i = z_i \sum_{j=1}^{n} W_{ij} z_j \tag{15}$$

where I_i is the local spatial relationship, and z_i and z_j are the normalized values of the variances.

Four clustering modes can be formed, and the LISA map formed from this can show the clustering characteristics. The clustering mode can be divided into H–H area, L–L area, L–H area, and H–L area.

5) Spatial Durbin Model: In the spatial econometric model, the spatial lag model assumes that all explanatory variables in the model will directly act on the dependent variables through the spatial conduction mechanism. The spatial error model assumes that the error term is the source of spatial interaction effects and that the spatial spillover effects formed by regions are caused by random shocks [54]. In the SDM, the dependent variable is affected by not only the spatial lag term and exogenous variable but also the lag term of the exogenous variable. The model expression is [55]

$$Y = \rho \boldsymbol{W} y + \theta \boldsymbol{W} x + Bx + \varepsilon \tag{16}$$

where ρ is the spillover effect value of the spatial element; $\boldsymbol{W}y$ is the spatial lag term of the explained variable; $\theta \boldsymbol{W}x$ is the spatial lag term of the explanatory variable; B is the coefficient of the explanatory variable; and ε is a random error item. The spatial weight matrix is determined by the proximity criterion.

III. RESULTS

A. Spatiotemporal Evolution of CESI

According to the AHP calculation formula, a judgment matrix of the CESI of the AALYR was constructed, and the weights of the seven types of ESs were obtained (see Table II).

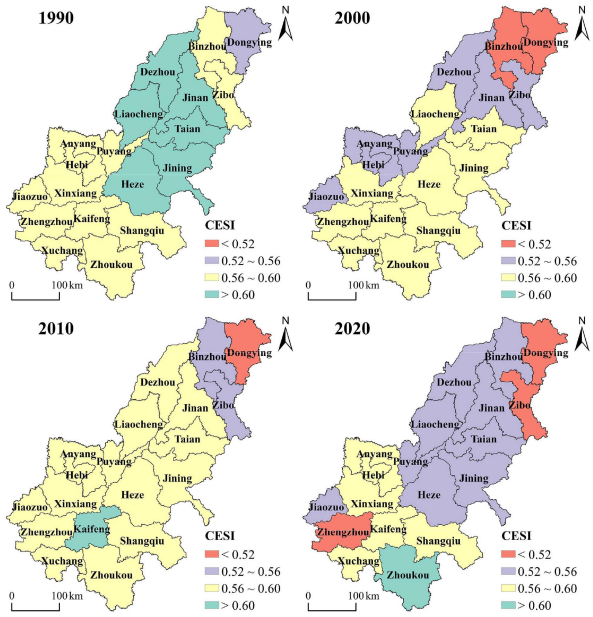

Fig. 4. Distribution of CESIs at city level from 1990 to 2020.

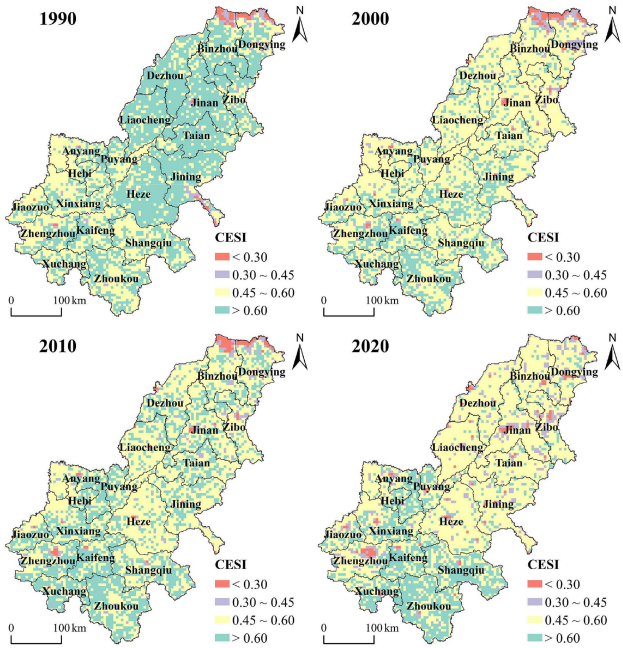

Fig. 5. Distribution of CESIs at grid scale from 1990 to 2020.

It can be seen from Table II that among the weights obtained through the judgment matrix, the food supply and habitat quality account for a relatively high proportion, 0.3076 and 0.3009, respectively, while the weights of other services are relatively low, and the results also pass the consistency test. Based on the weights of various ESs in Table II, combined with the normalized values of seven types of ESs on each grid, the spatial distribution of the CESI at the municipal and grid scales in the AALYR from 1990 to 2020 is obtained (see Figs. 4 and 5).

Fig. 4 shows that the CESI in the AALYR has a downward trend from 1990 to 2020. In 1990, the CESI of the study area

was relatively high, and the CESI of Shandong Province was higher than that of all cities in Henan Province, showing the distribution characteristic of high in the northeast. The cities with a composite index > 0.60 were in Shandong Province, namely Heze, Jining, Tai'an, Jinan, Dezhou, and Liaocheng. The composite index of most cities is in the range of 0.56–0.60, while the composite index of Dongying is the lowest, 0.53. In 2000, the CESI of the study area decreased significantly, and the index value of all cities was lower than 0.60. The number of cities falling below 0.56 has increased. The composite index of Dezhou, Jinan, Zibo, Puyang, Anyang, Hebi, and Jiaozuo is in the range of 0.52–0.56, and the composite index of Binzhou and Dongying has fallen below 0.52. The distribution characteristic of the CESI in this year changed from high in the northeast to high in the southwest. In 2010, ESs in the study area were improved as a whole, and the composite index of most cities increased. Among them, Kaifeng has the highest composite index and is also the only city above 0.60. The vast majority of urban CESI are still in the range of 0.56–0.60. Low-value areas are concentrated in the northeast region, while Dongying has the lowest composite index. In 2020, the CESI of the study area turned to a downward trend, and the distribution characteristics of high in the southwest are more obvious. In this year, only the composite index of Zhoukou exceeded 0.60, and the composite index of most cities was lower than 0.56, which was mainly distributed in Shandong Province in the northeast of the study area. Among them, the composite index of Zhengzhou, Dongying, and Zibo was lower than 0.52.

It can be seen from Fig. 5 that the interannual difference of the CESI in the AALYR from 1990 to 2020 on the grid scale is also very significant. In 1990, the grid with a CESI value > 0.60 accounted for a relatively high proportion. It was in a large centralized distribution in the northeast of the study area and distributed more in the southwest, but it was relatively scattered, so it had the distribution characteristic of high in the northeast. In 2000, the number of grids with CESI value > 0.60 decreased significantly. The northeast region changed significantly, while the distribution of high-value areas in the southwest changed slightly. The CESI value of the grid in this year is mainly in the range of 0.45–0.60. The low-value grid was still mainly distributed in the coastal areas of Binzhou and Dongying. In 2010, the number of grids with CESI value > 0.60 increased in most cities, and the distribution pattern changed slightly. In 2020, the region with significant changes in the CESI was still the northeast region, showing a downward trend. The change in the southwest was weak, and the characteristic of high in the southwest was more significant. At the same time, the low-value areas showed an expanding trend. Among them, the low-value areas in Zhengzhou, Jinan, and Zibo were relatively concentrated, so their overall CESI was also low.

Table III presents that the I value of the CESI from 1990 to 2020 was positive. The I value decreased from 0.325 in 1990 to 0.306 in 2000, and then continued to decline to 0.292 in 2010. Although it rose in 2020, it was only 0.294, showing a downward trend during the study period. This shows that the CESI in the AALYR had a positive spatial correlation, but the degree of positive correlation showed a weakening trend.

TABLE III
GLOBAL SPATIAL CORRELATION OF CESI IN THE AALYR FROM 1990 TO 2020

Year	I	P
1990	0.325	0.000
2000	0.306	0.000
2010	0.292	0.000
2020	0.294	0.000

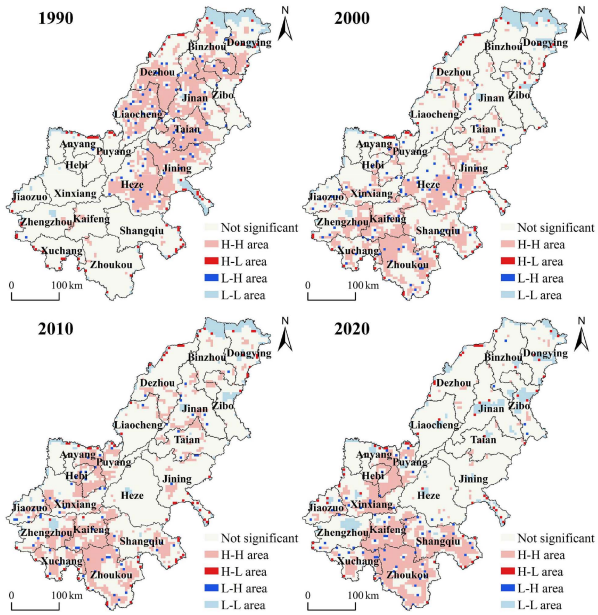

Fig. 6. Spatial distribution of CESIs from 1990 to 2020.

Based on calculating the global correlation, the local spatial autocorrelation characteristics of the CESI were analyzed by LISA diagram (see Fig. 6). Fig. 6 shows that the aggregation type of the CESI in the AALYR from 1990 to 2020 was mainly H–H area, followed by L–L area, and the distribution of H–L area and L–H area was very small. In 1990, a large area with a high value of the CESI was concentrated in the northeast region. Therefore, the area was mainly in the state of H–H aggregation.

The distribution pattern of aggregation types from 2000 to 2020 was relatively similar. Since the distribution characteristics of the CESI became high in the southwest, the high-value areas were mainly distributed in the southwest region, so the H–H aggregation from 2000 to 2020 was mainly distributed in the southwest region. There were also H–H clusters in the northeast region, but the overall trend was decreasing. L–L clusters were mainly distributed in Binzhou, Dongying, Jinan, Zibo, and Zhengzhou. Among them, there was a decreasing trend in Binzhou and Dongying, while the L–L clusters in Jinan, Zibo, and Zhengzhou showed a continuous expansion trend, indicating that their composite ESs have a negative transformation trend.

B. Correlation Analysis of CESI

We reflected the overall urbanization level using population density (PD), economic density (ED), and land development degree (LD). The spatial association results are shown in Table IV.

TABLE IV
GLOBAL STATISTICAL VALUE OF CESI AND URBANIZATION INDEX FROM 1990 TO 2020

I	1990	2000	2010	2020
PD	0.15	0.13	0.02	−0.09
ED	0.30	−0.01	−0.02	−0.15
LD	0.01	−0.04	−0.12	−0.12

Table IV presents that Moran's I between the CESI and population density, economic density, and land development degree in the AALYR from 1990 to 2020 has changed from positive to negative, but there were differences in the evolution process. In 1990, Moran's I between the CESI and the three urbanization indicators was positive, of which the ED had the highest positive correlation, reaching 0.30, followed by the PD, 0.15, and the LD had a weak positive correlation, only 0.01. It shows that the CESI of the surrounding areas with high PD and ED in the AALYR in this year was also relatively high, while the impact of LD on the CESI was small. In 2000, the I value of PD changed slightly and still had a significant positive correlation, while the I value of ED and LD became negative, but only -0.01 and -0.04, and the spatial negative correlation was weak. The I value of the three urbanization indicators continued to decrease in 2010. The I value of PD in this year was still positive, but only 0.02. The spatial positive correlation was weak, and the negative correlation of ED was also weak. The I value of LD decreased to -0.12, and the spatial negative correlation was gradually significant. In 2020, the I values of the three urbanization indicators became negative, and the I values of PD, ED, and LD were -0.09, -0.15, and -0.12, respectively, indicating that the spatial negative correlation between the CESI and urbanization indicators gradually became obvious, and the negative impact of urbanization process on the improvement of the CESI gradually increased.

To further explore the spatial correlation between the CESI and the urbanization index of the AALYR from 1990 to 2020, a LISA distribution map was obtained (see Fig. 7).

Fig. 7 shows that the CESI and urbanization indicators from 1990 to 2020 had significant spatial aggregation, but there were significant differences between the spatial distribution of PD, ED, and LD aggregation types. This is mainly due to the differences in the data dispersion range and spatial aggregation of the three urbanization indicators in the study area. There are significant differences in population density and economic density between regions, and the aggregation of high-value regions is more significant. In terms of PD, in 1990, the H–H area was widely distributed, mainly in Jinan, Jining, and Zhoukou, but it was mostly adjacent to the L–H area. The H–L and L–L areas were mainly distributed in Binzhou and Dongying in the northeast. In addition, there was also a small amount of distribution in Dezhou, Zibo, Jining, and Xinxiang. From 2000 to 2020, the aggregation effect continued to weaken, and the distribution areas of various aggregation types continued to decrease, with the most obvious reduction in the H–H area. H–L and L–L areas still basically maintained their distribution pattern, and

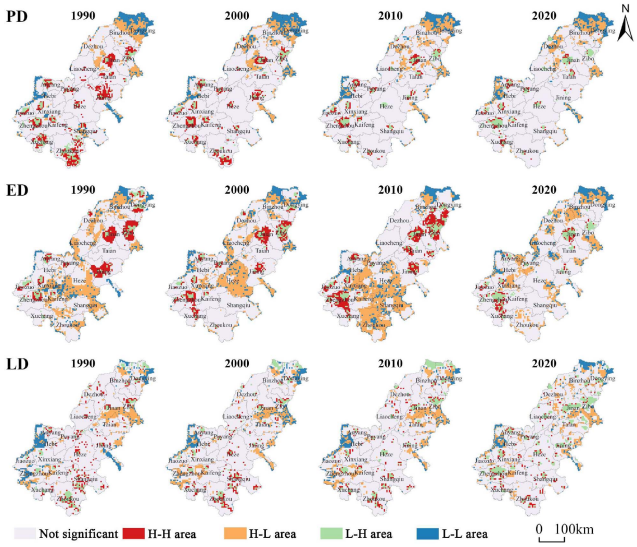

Fig. 7. Spatial correlation distribution of the CESI and urbanization indicators from 1990 to 2020.

L–H areas were gradually expanding in Zhengzhou, Jinan, and Zibo, so the overall spatial negative correlation was weak. In terms of ED, the existing aggregation types were mainly H–L and H–H areas. In 1990, the H–L area was widely distributed in the southwest region and in the northeast. The H–H area was mainly distributed in Jining, Jinan, and Zibo. From 1990 to 2010, H–H area and H–L area showed a trend of first shrinking adjacent to H–H area, and L–L area was adjacent to H–L area. In 2020, the H–H area was significantly reduced. The study area was mainly the H–L area, which was distributed in a small area in many cities. At the same time, the L–L area was still adjacent to it. The L–H area was mainly distributed in Zhengzhou, Jinan, and Zibo. In terms of LD, compared with PD and ED, the aggregate type distribution between the composite index and LD in 1990–2000 was less, mainly distributed in the H–L and L–L areas, and the spatial correlation was not significant. From 2010 to 2020, the L–H region continued to expand, and the distribution characteristics of other aggregation types changed slightly, so its spatial negative correlation gradually became significant.

C. Spatial Spillover Effects

After the model test and effect selection, the SDM model under individual fixed effect was selected to explore the impact mechanism and spatial effect of urbanization indicators on the CESI (see Table V). Table V presents that the absolute values of the indirect effects of the three urbanization indicators were greater than the direct effects, indicating that there was a large spillover effect in space, with spatial linkage. The direct and indirect effect coefficients of PD were both positive, 0.099 and 0.423, respectively, which had a weak positive impact on the local area but had a significant positive spatial spillover effect. The increase in population density may come from the increase in the scale of the local population, but it also includes the population that has migrated from other regions. This may mean that the population scale of neighboring areas will decrease,

TABLE V
SPATIAL SPILLOVER EFFECT OF URBANIZATION INDICATORS

Variable	Direct effect	Indirect effect	Total effect
PD	0.099**	0.423*	0.522*
	(0.04)	(0.08)	(0.06)
ED	−0.025***	0.076***	0.051***
	(0.01)	(0.00)	(0.00)
LD	−0.184***	−0.345**	−0.530***
	(0.00)	(0.03)	(0.00)

***, **, and * respectively represent $P < 0.01$, $P < 0.05$, and $P < 0.1$, the and specific P-value is shown in parentheses.

and the pressure on the ecosystem will also decrease, so the population density has a positive spillover effect. The direct effect of ED was negative, but the indirect effect was positive, indicating that it had a negative impact on the local CESI and a positive effect on the neighboring areas, but the total effect coefficient was only 0.051, which had a weak impact. The direct and indirect effect coefficients of LD were −0.184 and −0.345, respectively, which had a significant negative impact on the CESI of local and adjacent areas. On the one hand, it may be due to the existence of demonstration effects of land development. The increase in the degree of local land development may lead to increased land development efforts in adjacent areas, resulting in a negative impact on ESs. On the other hand, the construction materials used for regional land development may need to be supplied by other regions, which will affect the ecological environment of adjacent regions by affecting resource consumption and industrial production processes.

IV. DISCUSSION

This article calculates seven types of ESs and then constructs a CESI to analyze the space–time evolution characteristics of ESs in the AALYR from 1990 to 2020, and explores the spatial spillover effect of urbanization indicators on the CESI, which can provide support for the formulation of ecological construction policies in the region.

In this article, seven types of ESs in the AALYR from 1990 to 2020 were calculated by InVEST model and related methods. InVEST model has been widely used on different scales, and its reliability has been verified. It has good effect in analyzing the spatial characteristics of ESs [56]. Therefore, the InVEST model is selected in this article to calculate single ESs, which is convenient for spatial visualization. Natural processes and human activities often interact strongly in river basin areas and provide many important services, such as irrigating cultivated land, nourishing vegetation, and maintaining biodiversity [57], [58]. At the same time, the river basin is also a key area to ensure ecological security. However, facing the dual pressure of fragile ecological conditions and unreasonable human activities, it will face many ecological and environmental problems [59]. Therefore, the research on ESs in the basin area has become a rising research hotspot. This article enriches the research on ESs in the basin area.

Based on the calculation of the single ESs, the CESI is constructed by the AHP to evaluate the overall ESs in the AALYR. In the previous studies, the evaluation of the overall regional ESs level was mostly calculated by the equivalent factor method, which is convenient to obtain the total value of regional ESs [60]. However, the distribution pattern of ESs in this type of research is mainly determined by the land use in the study area. At the same time, the weight of various ESs cannot be adjusted according to the relative importance of single ESs in the study area. In comparison, based on considering land-use changes, we also add factors, such as terrain, precipitation, and evapotranspiration, to the impact of ESs, which relatively reduces the deviation between the spatial distribution results of ESs and the actual distribution characteristics, and determine the different weights of ESs by comparing their relative importance to each other. Scholars have carried out relevant research on the CESI [61], [62], but by comparison, the ESs selected in this article are more abundant, which can relatively more comprehensively evaluate the regional composite ESs.

In terms of the correlation between urbanization indicators and CESI, PD, ED, LD, and CESI have significant spatial correlation, which is as good as previous research results effect [63]. We found that PD has a significant positive effect on CESI based on the SDM. This is mainly because our research period began in 1990 when the population density in the study area was still low and continued to grow. Some scholars have found that when the regional PD is lower than a certain threshold, socioeconomic and ecological systems can develop together [64]. The spatial correlation changes between the two obtained in this article also verify the existence of the threshold, and the positive correlation has gradually decreased and eventually evolved into a negative correlation. Therefore, the positive effect obtained in this article only represents the overall situation during the research period, but if only the latest year is selected for spatial metrological analysis, it is likely to have a negative effect. At the same time, in terms of spatial distribution, the regions where the CESI and three urbanization indicators show L–H aggregation are also expanding in Zhengzhou, Jinan, and Zibo, which are also the regions with relatively high population scale and rapid socioeconomic development in the study area, indicating that they have exceeded the reasonable threshold. There is a negative spatial correlation between the CESI and the degree of LD, which is consistent with previous studies. Peng et al. [65] found that there is a negative linear relationship between LD and total ESs. Other major river basins in the world, such as the Yangtze River Basin, the Nile Basin, and the Amazon Basin, are areas of population and socioeconomic aggregation, and may also be experiencing rapid urban expansion. The natural environment and ecological functions of these watersheds will be affected by urbanization, and the spillover effects of urbanization indicators obtained have a certain reference value for their urbanization development policies.

Based on the above discussion, we put forward some policy recommendations.

1) Rationally regulate the population scale in areas with high PD. The low-value area of the CESI shows an obvious expansion trend in Zhengzhou and Jinan and other cities

with high PD. It is necessary to reasonably regulate its population scale and spatial distribution so that the ecosystem and social economy can develop together.

2) We need to promote land urbanization in an orderly manner. With the continuous expansion of built-up land, the pressure on the ecological environment is increasing, and there is a negative spatial spillover effect. Therefore, the ecological red line should be set according to the ecological carrying capacity, and the area of built-up land should be strictly controlled.
3) Break administrative boundaries, realize coordinated governance of inter-regional ecosystems, implement the system and mechanism of ecological linkage and protection cooperation between administrative boundaries, and promote regional sustainable development.

This article constructs a CESI by measuring seven types of ESs to evaluate the overall ESs in the AALYR. Compared with the separate evaluation of multiple types of ESs, it can more comprehensively evaluate the regional ESs' functions, but there are still some deficiencies. When using the InVEST model to calculate single ESs, some parameters need to be continuously adjusted according to the actual situation of the study area to select the optimal parameter values. This article also carried out a certain degree of experiments to determine the relatively more appropriate parameter values. However, according to the choice of data sources and the different number of experiments, there should be room for further adjustment so that the calculation results are more consistent with the actual situation. In future research, based on building the CESI, we will deeply analyze the tradeoff and synergy between various ESs, and more specifically explore the impact of single ESs on the evolution of composite ESs.

V. Conclusion

Watersheds generally have complex ecosystem structures, which are closely related to human production and activities, and are easy to cause changes in watershed ESs. We found that the CESI in the AALYR gradually changed from high in the northeast to high in the southwest from 1990 to 2020, and there were significant differences in the changing trend between the years. At the same time, the CESI has a significant positive spatial correlation but shows a weakening trend. In terms of the correlation with urbanization indicators, the relationship among CESI and PD, ED, and LD has changed from positive spatial correlation to negative spatial correlation, but there are differences in the evolution process and spatial distribution of aggregation types. In terms of spatial spillover effect, there are significant differences among the three urbanization indicators. PD has a positive spillover effect on the CESI, and LD has a significant negative spillover effect. ED has a weak positive spillover effect overall.

Acknowledgment

The authors would like to thank the Geographical Science Data Center of The Greater Bay Area for providing the relevant data in this study.

References

[1] M. C. Urban, "Accelerating extinction risk from climate change," *Science*, vol. 348, no. 6234, pp. 571–573, May 2015, doi: 10.1126/science.aaa4984.
[2] P. T. Brown and K. Caldeira, "Greater future global warming inferred from Earth's recent energy budget," *Nature*, vol. 552, no. 7683, pp. 45–50, Dec. 2017, doi: 10.1038/nature24672.
[3] M. Burke, S. M. Hsiang, and E. Miguel, "Global non-linear effect of temperature on economic production," *Nature*, vol. 527, no. 7577, pp. 235–239, Nov. 2015, doi: 10.1038/nature15725.
[4] S. R. Weiskopf et al., "Climate change effects on biodiversity, ecosystems, ecosystem services, and natural resource management in the United States," *Sci. Total Environ.*, vol. 733, Sep. 2020, Art. no. 137782, doi: 10.1016/j.scitotenv.2020.137782.
[5] L. Mandle et al., "Increasing decision relevance of ecosystem service science," *Nature Sustain.*, vol. 4, no. 2, pp. 161–169, Oct. 2020, doi: 10.1038/S41893-020-00625-Y.
[6] Y. Zhang, H. Balzter, B. Liu, and Y. Chen, "Analyzing the impacts of urbanization and seasonal variation on land surface temperature based on subpixel fractional covers using Landsat images," *IEEE J. Sel. Topics Appl. Earth Observ. Remote Sens.*, vol. 4, no. 2, pp. 1344–1356, Apr. 2017, doi: 10.1109/JSTARS.2016.2608390.
[7] H. M. Liu, L. Xing, C. X. Wang, and H. Y. Zhang, "Sustainability assessment of coupled human and natural systems from the perspective of the supply and demand of ecosystem services," *Front. Earth Sci.*, vol. 10, Oct. 2022, Art. no. 1025787, doi: 10.3389/feart.2022.1025787.
[8] R. S. De Groot, M. A. Wilson, and R. M. J. Boumans, "A typology for the classification, description and valuation of ecosystem functions, goods and services," *Ecol. Econ.*, vol. 41, no. 3, pp. 393–408, Jun. 2002, doi: 10.1016/S0921-8009(02)00089-7.
[9] R. Costanza et al., "The value of the world's ecosystem services and natural capital," *Nature*, vol. 387, no. 6630, pp. 253–260, May 1997, doi: 10.1038/387253a0.
[10] Q. Wei, L. J. Tong, J. Gondwe, X. G. Lv, W. M. Tong, and Y. Liu, "Non-use value trends analysis of wetland ecosystem in the Sanjiang Plain, Northeast China," *Wetlands Ecol. Manage.*, vol. 23, no. 3, pp. 347–355, Sep. 2015, doi: 10.1007/s11273-014-9384-0.
[11] M. D. Davidson, "On the relation between ecosystem services, intrinsic value, existence value and economic valuation," *Ecol. Econ.*, vol. 95, pp. 171–177, Nov. 2013, doi: 10.1016/j.ecolecon.2013.09.002.
[12] P. C. Sutton and R. Costanza, "Global estimates of market and non-market values derived from nighttime satellite imagery, land cover, and ecosystem service valuation," *Ecol. Econ.*, vol. 41, no. 3, pp. 509–527, Jun. 2002, doi: 10.1016/S0921-8009(02)00097-6.
[13] A. A. Shedayi, M. Xu, J. Gonalez-Redin, A. Ali, L. Shahzad, and S. Rahim, "Spatiotemporal valuation of cultural and natural landscapes contributing to Pakistan's cultural ecosystem services," *Environ. Sci. Pollut. Res.*, vol. 29, no. 27, pp. 41834–41848, Jan. 2022, doi: 10.1007/S11356-021-17611-2.
[14] H. Yu, J. Yang, D. Sun, T. Li, and Y. Liu, "Spatial responses of ecosystem service value during the development of urban agglomerations," *Land*, vol. 11, no. 2, Feb. 2022, Art. no. 165, doi: 10.3390/land11020165.
[15] Z. Y. Wang and J. S. Cao, "Assessing and predicting the impact of multi-scenario land use changes on the ecosystem service value: A case study in the upstream of Xiong'an New Area, China," *Sustainability*, vol. 13, no. 2, pp. 704–704, Jan. 2021, doi: 10.3390/SU13020704.
[16] J. W. Redhead et al., "Empirical validation of the InVEST water yield ecosystem service model at a national scale," *Sci. Total Environ.*, vol. 569/570, pp. 1418–1426, Nov. 2016, doi: 10.1016/j.scitotenv.2016.06.227.
[17] J. Gao, F. Li, H. Gao, C. B. Zhou, and X. L. Zhang, "The impact of land-use change on water-related ecosystem services: A study of the Guishui River Basin, Beijing, China," *J. Cleaner Prod.*, vol. 163, pp. 148–155, Oct. 2017, doi: 10.1016/j.jclepro.2016.01.049.
[18] J. Haas and Y. Ban, "Mapping and monitoring urban ecosystem services using multitemporal high-resolution satellite data," *IEEE J. Sel. Topics Appl. Earth Observ. Remote Sens.*, vol. 10, no. 2, pp. 669–680, Feb. 2017, doi: 10.1109/JSTARS.2016.2586582.
[19] T. Ala-Hulkko, O. Kotavaara, J. Alahuhta, and J. Hjort, "Mapping supply and demand of a provisioning ecosystem service across Europe," *Ecol. Indicators*, vol. 103, pp. 520–529, Aug. 2019, doi: 10.1016/j.ecolind.2019.04.049.
[20] M. Sharafatmandrad and A. K. Mashizi, "Temporal and spatial assessment of supply and demand of the water-yield ecosystem service for water scarcity management in arid to semi-arid ecosystems," *Water Resour. Manage.*, vol. 35, pp. 63–82, Nov. 2021, doi: 10.1007/s11269-020-02706-1.

[21] A. Woldeyohannes, M. Cotter, W. D. Biru, and G. Kelboro, "Assessing changes in ecosystem service values over 1985–2050 in response to land use and land cover dynamics in Abaya-Chamo Basin, Southern Ethiopia," *Land*, vol. 9, no. 2, Jan. 2020, Art. no. 37, doi: 10.3390/land9020037.

[22] D. Richards et al., "Global variation in climate, human development, and population density has implications for urban ecosystem services," *Sustainability*, vol. 11, no. 22, pp. 6200–6200, Nov. 2019, doi: 10.3390/su11226200.

[23] J. Fu, Q. Zhang, P. Wang, L. Zhang, Y. Q. Tian, and X. R. Li, "Spatiotemporal changes in ecosystem service value and its coordinated development with economy: A case study in Hainan Province, China," *Remote Sens.*, vol. 14, no. 4, pp. 970–970, Feb. 2022, doi: 10.3390/RS14040970.

[24] J. Haas and Y. Ban, "Urban land cover and ecosystem service changes based on Sentinel-2A MSI and Landsat TM data," *IEEE J. Sel. Topics Appl. Earth Observ. Remote Sens.*, vol. 11, no. 2, pp. 485–497, Feb. 2018, doi: 10.1109/JSTARS.2017.2786468.

[25] L. Hein, L. White, A. Miles, and P. Roberts, "Analysing the impacts of air quality policies on ecosystem services: A case study for Telemark, Norway," *J. Environ. Manage.*, vol. 206, pp. 650–663, Jan. 2018, doi: 10.1016/j.jenvman.2017.10.073.

[26] L. J. Wang, S. Ma, J. Jiang, Y. G. Zhao, and J. C. Zhang, "Spatiotemporal variation in ecosystem services and their drivers among different landscape heterogeneity units and terrain gradients in the southern hill and mountain belt, China," *Remote Sens.*, vol. 13, no. 7, pp. 1375–1375, Apr. 2021, doi: 10.3390/RS13071375.

[27] R. F. Bangash et al., "Ecosystem services in Mediterranean river basin: Climate change impact on water provisioning and erosion control," *Sci. Total Environ.*, vol. 458–460, pp. 246–255, Aug. 2013, doi: 10.1016/j.scitotenv.2013.04.025.

[28] T. Zhou, H. Liu, P. Gou, and N. Xu, "Conflict or coordination? Measuring the relationships between urbanization and vegetation cover in China," *Ecol. Indicators*, vol. 147, Mar. 2023, Art. no. 109993, doi: 10.1016/J.ECOLIND.2023.109993.

[29] W. L. Geng, Y. Y. Li, P. Y. Zhang, D. Yang, W. L. Jing, and T. Q. Rong, "Analyzing spatio-temporal changes and trade-offs/synergies among ecosystem services in the Yellow River Basin, China," *Ecol. Indicators*, vol. 138, May 2022, Art. no. 108825, doi: 10.1016/J.ECOLIND.2022.108825.

[30] C. Lu, M. Hou, Z. Liu, H. Li, and C. Lu, "Variation Characteristic of NDVI and its response to climate change in the middle and upper reaches of Yellow River Basin, China," *IEEE J. Sel. Topics Appl. Earth Observ. Remote Sens.*, vol. 14, pp. 8484–8496, Aug. 2021, doi: 10.1109/JSTARS.2021.3105897.

[31] J. X. Sun, M. Han, F. B. Kong, F. Wei, and X. L. Kong, "Spatiotemporal analysis of the coupling relationship between habitat quality and urbanization in the lower Yellow River," *Int. J. Environ. Res. Public Health*, vol. 20, no. 6, Mar. 2023, Art. no. 4734, doi: 10.3390/ijerph20064734.

[32] G. T. Yu et al., "Impact of land use/land cover change on ecological quality during urbanization in the lower Yellow River Basin: A case study of Jinan City," *Remote Sens.*, vol. 14, no. 24, Dec. 2022, Art. no. 6273, doi: 10.3390/rs14246273.

[33] D. Yang, P. Y. Zhang, L. Jiang, Y. Zhang, Z. Y. Liu, and T. Q. Rong, "Spatial change and scale dependence of built-up land expansion and landscape pattern evolution—Case study of affected area of the lower Yellow River," *Ecol. Indicators*, vol. 141, Aug. 2022, Art. no. 109123, doi: 10.1016/J.ECOLIND.2022.109123.

[34] Y. Zhang et al., "Dynamic changes, spatiotemporal differences and factors influencing the urban eco-efficiency in the lower reaches of the Yellow River," *Int. J. Environ. Res. Public Health*, vol. 17, no. 20, Oct. 2020, Art. no. 7510, doi: 10.3390/ijerph17207510.

[35] S. Z. Peng, Y. X. Ding, W. Z. Liu, and Z. Li, "1 km monthly temperature and precipitation dataset for China from 1901 to 2017," *Earth Syst. Sci. Data*, vol. 11, pp. 1931–1946, Dec. 2019, doi: 10.5194/essd-11-1931-2019.

[36] Y. Ding and S. Peng, "Spatiotemporal change and attribution of potential evapotranspiration over China from 1901 to 2100," *Theor. Appl. Climatol.*, vol. 145, no. 12, pp. 79–94, Apr. 2021, doi: 10.1007/S00704-021-03625-W.

[37] L. X. Zhang, Z. H. Ren, B. Chen, P. Gong, H. H. Fu, and B. Xu, "A prolonged artificial nighttime-light dataset of China (1984–2020)," *Big Earth Data Platform Three Poles*, 2021, doi: 10.11888/Socioeco.tpdc.271202.

[38] N. F. Wang, X. P. Chen, Z. L. Zhang, and J. X. Pang, "Spatiotemporal dynamics and driving factors of county-level carbon storage in the Loess Plateau: A case study in Qingcheng County, China," *Ecol. Indicators*, vol. 144, Nov. 2022, Art. no. 109460, doi: 10.1016/J.ECOLIND.2022.109460.

[39] J. Y. Li, J. Gong, J. M. Guldmann, S. C. Li, and J. Zhu, "Carbon dynamics in the northeastern Qinghai–Tibetan plateau from 1990 to 2030 using Landsat land use/cover change data," *Remote Sens.*, vol. 12, no. 3, pp. 528–528, Feb. 2020, doi: 10.3390/rs12030528.

[40] W. F. Gong et al., "Assessing the impact of land use and changes in land cover related to carbon storage by linking trajectory analysis and InVEST models in the Nandu River Basin on Hainan Island in China," *Front. Environ. Sci.*, vol. 10, Oct. 2022, Art. no. 1038752, doi: 10.3389/FENVS.2022.1038752.

[41] Q. L. Zhang and K. C. Seto, "Mapping urbanization dynamics at regional and global scales using multi-temporal DMSP/OLS nighttime light data," *Remote Sens. Environ.*, vol. 115, no. 9, pp. 2320–2329, Sep. 2011, doi: 10.1016/j.rse.2011.04.032.

[42] M. Moreira, C. Fonseca, M. Vergilio, H. Calado, and A. Gil, "Spatial assessment of habitat conservation status in a Macaronesian island based on the InVEST model: A case study of Pico Island (Azores, Portugal)," *Land Use Policy*, vol. 78, pp. 637–649, Nov. 2018, doi: 10.1016/j.landusepol.2018.07.015.

[43] A. Al Kafy et al., "Integrating forest cover change and carbon storage dynamics: Leveraging Google Earth engine and InVEST model to inform conservation in hilly regions," *Ecol. Indicators*, vol. 152, Aug. 2023, Art. no. 110374, doi: 10.1016/j.ecolind.2023.110374.

[44] W. M. Hu, G. Li, Z. H. Gao, G. Y. Jia, Z. C. Wang, and Y. Li, "Assessment of the impact of the poplar ecological retreat project on water conservation in the Dongting Lake wetland region using the InVEST model," *Sci. Total Environ.*, vol. 733, Sep. 2020, Art. no. 139423, doi: 10.1016/j.scitotenv.2020.139423.

[45] X. Duolaiti, A. Kasimu, R. Reheman, Y. Aizizi, and B. Wei, "Assessment of water yield and water purification services in the arid zone of Northwest China: The case of the Ebinur Lake Basin," *Land*, vol. 12, no. 3, Mar. 2023, Art. no. 533, doi: 10.3390/land12030533.

[46] J. Zhao, Z. Shao, C. Y. Xia, K. Fang, R. Chen, and J. Zhou, "Ecosystem services assessment based on land use simulation: A case study in the Heihe River Basin, China," *Ecol. Indicators*, vol. 143, Oct. 2022, Art. no. 109402, doi: 10.1016/j.ecolind.2022.109402.

[47] J. J. Tang et al., "Impacts and predictions of urban expansion on habitat quality in the densely populated areas: A case study of the Yellow River Basin, China," *Ecol. Indicators*, vol. 151, Jul. 2023, Art. no. 110320, doi: 10.1016/j.ecolind.2023.110320.

[48] J. M. Liu, X. T. Pei, W. Y. Zhu, and J. Z. Jiao, "Understanding the intricate tradeoffs among ecosystem services in the Beijing-Tianjin-Hebei urban agglomeration across spatiotemporal features," *Sci. Total Environ.*, vol. 898, Jul. 2023, Art. no. 165453, doi: 10.1016/j.scitotenv.2023.165453.

[49] N. H. Pan, Q. Y. Guan, Q. Z. Wang, Y. F. Sun, H. C. Li, and Y. R. Ma, "Spatial differentiation and driving mechanisms in ecosystem service value of arid region: A case study in the middle and lower reaches of Shule River Basin, NW China," *J. Cleaner Prod.*, vol. 319, Oct. 2021, Art. no. 128718, doi: 10.1016/j.jclepro.2021.128718.

[50] A. Petrillo, F. Colangelo, I. Farina, M. Travaglioni, C. Salzano, and R. Cioffi, "Multi-criteria analysis for life cycle assessment and life cycle costing of lightweight artificial aggregates from industrial waste by double-step cold bonding palletization," *J. Cleaner Prod.*, vol. 351, Jun. 2022, Art. no. 131395, doi: 10.1016/J.JCLEPRO.2022.131395.

[51] L. Liang, X. Z. Deng, P. Wang, Z. H. Wang, and L. S. Wang, "Assessment of the impact of climate change on cities livability in China," *Sci. Total Environ.*, vol. 726, Jul. 2020, Art. no. 138339, doi: 10.1016/j.scitotenv.2020.138339.

[52] L. Anselin, "Local indicators of spatial association: LISA," *Geograph. Anal.*, vol. 27, no. 2, pp. 93–115, Apr. 1995, doi: 10.1111/j.1538-4632.1995.tb00338.x.

[53] W. Y. Qiao and X. J. Huang, "The impact of land urbanization on ecosystem health in the Yangtze River Delta urban agglomerations, China," *Cities*, vol. 130, Nov. 2022, Art. no. 103981, doi: 10.1016/J.CITIES.2022.103981.

[54] H. Y. Liu and Y. R. Song, "Financial development and carbon emissions in China since the recent world financial crisis: Evidence from a spatial-temporal analysis and a spatial Durbin model," *Sci. Total Environ.*, vol. 715, May 2020, Art. no. 136771, doi: 10.1016/j.scitotenv.2020.136771.

[55] P. J. Zhao, L. E. Zeng, H. Y. Lu, Y. Zhou, H. Y. Hu, and X. Y. Wei, "Green economic efficiency and its influencing factors in China from 2008 to 2017: Based on the super-SBM model with undesirable outputs and spatial Durbin model," *Sci. Total Environ.*, vol. 741, Nov. 2020, Art. no. 140026, doi: 10.1016/j.scitotenv.2020.140026.

[56] X. Y. Sun, R. F. Shan, and F. Liu, "Spatio-temporal quantification of patterns, trade-offs and synergies among multiple hydrological ecosystem services in different topographic basins," *J. Cleaner Prod.*, vol. 268, Sep. 2020, Art. no. 122338, doi: 10.1016/j.jclepro.2020.122338.

[57] L. B. Ma, J. Bo, X. Y. Li, F. Fang, and W. J. Cheng, "Identifying key landscape pattern indices influencing the ecological security of inland river basin: The middle and lower reaches of Shule River Basin as an example," *Sci. Total Environ.*, vol. 674, pp. 424–438, Jul. 2019, doi: 10.1016/j.scitotenv.2019.04.107.

[58] I. Khan, M. J. Zhao, S. U. Khan, L. Y. Yao, A. Ullah, and T. Xu, "Spatial heterogeneity of preferences for improvements in river basin ecosystem services and its validity for benefit transfer," *Ecol. Indicators*, vol. 93, pp. 627–637, Oct. 2018, doi: 10.1016/j.ecolind.2018.05.018.

[59] M. M. Gou et al., "Integrating ecosystem service trade-offs and rocky desertification into ecological security pattern construction in the Daning river basin of Southwest China," *Ecol. Indicators*, vol. 138, May 2022, Art. no. 108845, doi: 10.1016/J.ECOLIND.2022.108845.

[60] W. Song and X. Z. Deng, "Land-use/land-cover change and ecosystem service provision in China," *Sci. Total Environ.*, vol. 576, pp. 705–719, Jan. 2017, doi: 10.1016/j.scitotenv.2016.07.078.

[61] L. L. Wu and F. L. Fan, "Assessment of ecosystem services in new perspective: A comprehensive ecosystem service index (CESI) as a proxy to integrate multiple ecosystem services," *Ecol. Indicators*, vol. 138, May 2022, Art. no. 108800, doi: 10.1016/J.ECOLIND.2022.108800.

[62] Y. Q. Lang and W. Song, "Quantifying and mapping the responses of selected ecosystem services to projected land use changes," *Ecol. Indicators*, vol. 102, pp. 186–198, Jul. 2019, doi: 10.1016/j.ecolind.2019.02.019.

[63] C. X. Deng et al., "Spatiotemporal dislocation of urbanization and ecological construction increased the ecosystem service supply and demand imbalance," *J. Environ. Manage.*, vol. 288, Jun. 2021, Art. no. 112478, doi: 10.1016/J.JENVMAN.2021.112478.

[64] Z. T. Liu, R. Wu, Y. X. Chen, C. L. Fang, and S. J. Wang, "Factors of ecosystem service values in a fast-developing region in China: Insights from the joint impacts of human activities and natural conditions," *J. Cleaner Prod.*, vol. 297, May 2021, Art. no. 126588, doi: 10.1016/J.JCLEPRO.2021.126588.

[65] J. Peng, L. Tian, Y. X. Liu, M. Y. Zhao, Y. N. Hu, and J. S. Wu, "Ecosystem services response to urbanization in metropolitan areas: Thresholds identification," *Sci. Total Environ.*, vol. 607/608, pp. 706–714, Dec. 2017, doi: 10.1016/j.scitotenv.2017.06.218.

Zhenyue Liu received the B.S. degree in human geography and urban rural planning in 2020 from Henan University, Kaifeng, China, where he is currently working toward the Ph.D. degree in physical geography with the College of Geography and Environmental Science.

His research interests include land use change and ecosystem services.

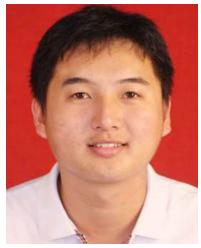

Pengyan Zhang received the Ph.D. degree in environmental geography from Henan University, Kaifeng, China, in 2013.

He is currently a Professor with the College of Urban Economics and Public Management, Capital University of Economics and Business, Beijing, China. His research interests mainly focus on land resource utilization and regional environmental governance.

Guanghui Li received the B.S. degree in electronic commerce from Xinyang Agriculture and Forestry University, Xinyang, China, in 2022. He is currently working toward the Ph.D. degree.

His research interest mainly focuses on sustainable land use.

Dan Yang received the M.S. degree in land resource management in 2019 from Henan University, Kaifeng, China, where she is currently working toward the Ph.D. degree in physical geography with the College of Geography and Environmental Science.

Her research interests mainly focus on land use and landscape patterns.

Mingzhou Qin received the Ph.D. degree in natural resources from Nanjing University, Nanjing, China, in 1995.

He is currently a Professor with the College of Geography and Environmental Science, Henan University, Kaifeng, China. His research interests mainly focus on land resource utilization and management, and land risk assessment.